RSC Advances

ROYAL SOCIETY OF CHEMISTRY

www.rsc.org/advances

Cite this: DOI: 10.1039/c0xx00000x

www.rsc.org/xxxxxx

PAPER

Hydrothermal synthesis of bimodal mesoporous MoS_2 nanosheets and their hydrodeoxygenation properties

Weiyan Wang,[a, b] * Lu Li,[a] Kui Wu,[a] Guohua Zhu,[a] Song Tan,[a] Wensong Li,[a] Yunquan Yang[a, b] *

Received (in XXX, XXX) Xth XXXXXXXXX 20XX, Accepted Xth XXXXXXXXX 20XX

DOI: 10.1039/b000000x

In this study, bimodal mesoporous MoS_2 nanosheets were successfully synthesized by hydrothermal method. The effect of pH value, pressure, time and temperature in the preparation process of MoS_2 on its structure property and catalytic activity were studied in detail. Low pH value and pressure were beneficial for the preparation of MoS_2 nanosheet with a large surface area and narrow bimodal pore distribution, which exposed more effective active sites on the surface and provided suitable space for reactants and products to diffuse in less resistance. But the acceleration hydrolysis of $CS(NH_2)_2$ at the low pH value enhanced the formation rate of MoS_2 and then weakened the nanosheet structure. In the HDO of *p*-cresol, MoS_2 exhibited high catalytic activity, and the dominant route was direct deoxygenation. After 4 h, both the conversion and deoxygenation degree reached to 99.9% at 300 °C, and toluene selectivity was 66.2%. The HDO reaction mechanism could be well explained by Rim−Edge model. The higher conversion in the HDO of *p*-cresol on MoS_2 depended on the larger surface area and more big pores of the catalyst, while the higher direct deoxygenation activity of MoS_2 depended on the more layers in its stacks.

1. Introduction

Up to now, fossil fuels are still the major energy resource in our society. Unfortunately, their reserve was declining and their utilizations produced much greenhouse gas and other poisonous gases, resulting in some serious environmental pollution problems, which stimulated us to explore renewable resources.[1] Bio-oil, derived from the fast pyrolysis of biomass under the conditions of isolated from oxygen and high temperature, has been considered as an ideal renewable substituted energy to reduce reliance on limited fossil fuels because of its carbon neutrality, enormous potential to deliver many forms of energy and numbers of organic chemicals.[2] However, the liquid fuel from lignin was consist of many oxygen-containing compounds such as phenols, alcohols and ketones, leading to the low heating value, highly corrosive and immiscibility with petroleum fuels. Consequently, this liquid fuel was difficult to be directly used as a supplement or replacement for gasoline or fossil diesel.[3] To address this problem, hydrodeoxygenation (HDO) was a propitious technology to be adopted to remove the oxygen from bio-oil.

In the past decade years, much effort had been devoted to the preparation of high HDO activity catalyst.[4-8] There had appeared several kinds of HDO catalysts, including sulphides,[7, 9-11] noble metals,[12-14] non-noble metals,[15-17] phosphides,[18, 19] borides,[20, 21] carbides[22] and ionic liquids.[23] Unfortunately, these catalysts had some disadvantages such as high cost, low activity or instability, which needed to be further improved. Sulphides had been widely studied in the hydrodesulfurization (HDS) reactions and exhibited high catalytic activity. Because of the similarity of HDS and HDO, sulphides had been also employed for the HDO reaction. However, the HDO activity of sulphides was closely relate to its preparation method. For example, K.J. Smith et al.[24] had compared the commercial MoS_2 with exfoliated MoS_2 and MoS_2 prepared by in situ decomposition of ammonium heptamolybdate or molybdenum naphthenate on the catalytic activity in the HDO of phenols and found that their activity was changed with its preparation method. C. Wang et al.[25] had prepared Ni-Mo-W-S trimetallic sulfide catalysts by a mechanical activation method and obtained a conversion of 97.8% in the HDO of *p*-cresol over these catalysts at 300 °C for 5 h. B. Yoosuk et al.[26] had prepared amorphous MoS_2 from ammonium tetrathiomolybdate by the hydrothermal method and reported that the conversion in the HDO of phenol on the prepared MoS_2 was 71% at 350 °C for 1 h. Recently, we had also adopted hydrothermal method to prepare MoS_2 using ammonium heptamolybdate and thiourea as raw materials and verified that adding surfactant during its preparation produced positive influence on its surface area and HDO activity.[27]

Although MoS_2 catalyst with high surface area has been prepared by hydrothermal method, its pore size distribution was very broad and displays a lot of small pores, which reduced its catalytic activity.[26] Bimodal pore structure had been found to be a key feature in hydrotreating processes, where the smaller pores provided the high surface area to expose more active sites while the larger pores provided the suitable space to decrease the mass transfer resistance for bulky reactant and product molecules.[28-30] Thus, a facile synthesis route for bimodal mesoporous MoS_2 was very interesting. Inspired by the synthesis of MoS_2 by hydrothermal method,[31-33] we changed the reaction conditions and successfully prepared bimodal mesoporous MoS_2 nanosheet

in this study. We concentrated on the effect of the preparation conditions such as pH value, reaction time, temperature on the structure of MoS_2 and their catalytic activity in the HDO of *p*-cresol.

2. Experimental section

2.1 Catalyst preparation

All solvents and reagents were obtained from Sinopharm Chemical Reagent Co., Ltd. in high purity (≥99%) and used without further purification. MoS_2 catalysts were prepared by a hydrothermal method. The catalyst synthesis was carried out in quartz reactor with a volume of 300 mL. Ammonium heptamolybdate (2.3 g) and thiourea (3.0 g) were dissolved in water and hydrochloric acid was added to adjust its pH value. Then, this mixed solution was added into the sealed reactor and heated for different time. After reaction, the resultant catalysts were separated and washed with water and ethanol for several times. Finally, the resulting product was dried under vacuum at 60 °C for 8 hours and stored in nitrogen environment. Corresponding names of the samples prepared under different conditions are listed in table 1.

Table 1 Corresponding names of the samples prepared under different conditions

Samples	Time (h)	pH	Pres. (MPa)	Temp. (°C)
Mo-S-1	12	1.4	2.3	200
Mo-S-2	12	0.9	2.3	200
Mo-S-3	12	0.7	2.3	200
Mo-S-4	12	1.4	1.5	200
Mo-S-5	12	0.9	1.5	200
Mo-S-6	12	0.7	1.5	200
Mo-S-7	12	0.9	3.5	240
Mo-S-8	24	0.9	3.5	240
Mo-S-9	36	0.9	3.5	240

2.2 Catalyst characterization

X-ray diffraction (XRD) measurements were carried on a D/max2550 18KW Rotating anode X-Ray Diffractometer with monochromatic Cu Kα radiation (λ= 1.5418Å) radiation at voltage and current of 40 kV and 300 mA. The 2θ was scanned over the range of 5-90° at a rate of 10°/min. The specific surface area was measured by a Quantachrome's NOVA-2100e Surface Area instrument by physisorption of nitrogen at -196 °C. The samples were dehydrated at 300 °C using vaccum degassing for 12 h before determination. The scanning electronic microscopy (SEM) images of the catalysts were obtained on a JEOL JSM-6360 electron microscopy. The micro-morphology of the prepared catalyst was measured by high resolution transmission electron microscopy (HRTEM) on a JEOL JEM-2100 transmission electron microscope with a lattice resolution of 0.19 nm and an accelerating voltage of 200 kV. The samples for the HRTEM study were prepared by the ultrasonic dispersing in ethanol and consequent deposition of the suspension upon a "holey" carbon film supported on a copper grid. The samples were kept under inert atmosphere until the last process.

2.3 Catalyst activity measurement

The HDO activity tests were carried out in a 300-mL sealed autoclave. The prepared catalyst without any further treatment (0.60 g), *p*-cresol (13.50 g) and dodecane (86.20 g) were placed into the autoclave. Air in the autoclave was evacuated by pressurization-depressurization cycles with nitrogen and subsequently with hydrogen. The system was heated to 300 °C, then pressurized with hydrogen to 4.0 MPa and adjusted the stirring speed to 900 rpm. During the reaction, liquid samples were withdrawn from the reactor and analyzed by Agilent 6890/5973N GC-MS and 7890 gas chromatography using a flame ionization detector (FID) with a 30 m AT-5 capillary column. To separate the reaction products, the temperature in the GC oven was heated from 40 °C to 85 °C with the ramp of 20 °C/min, held at 85 °C for 4.0 min, then heated to 200 °C at a rate of 20 °C/min and kept at 200 °C for 5.0 min. Internal standards (i.e., octane for methylcyclohexane, toluene and decane for *p*-cresol) were used to determine the product distribution and carbon balance. These experiments have been repeated twice at least and the results showed that the conversion and selectivity were within 3.0% of the average values. HYD/DDO is defined as (Total selectivity of methylcyclohexane and 3-methylcyclohexene)/the selectivity of toluene; Deoxygenation degree (D. D., wt %) is defined as [1-oxygen content in the final organic compounds / total oxygen content in the initial material] × 100%. Carbon balance is better than 96 ± 3 % in this work.

3. Results and discussion

3.1 Synthesis of MoS_2

G. R. Helz et al.[34] had found that pH value over the course of the reactions significantly increased owing to H_2S consumption and the step of formation of MoS_3 was so slow that very little MoS_3 produced without acid catalysis. E. H. Lester et al.[35] had also reported it is necessary to add acid to provide an acidic environment to produce MoS_3. Y Piao et al.[31] had also verified that the H^+ ions from the hydrochloric acid play a catalytic role in the formation of MoS_2 during the hydrothermal process. Consequently, according to above previous reports [31, 34, 35] and the experimental conditions for the preparation of MoS_2 in this study, the formation of MoS_2 involved a complex process and contained four steps: (1) the hydrolysis of $CS(NH_2)_2$, (2) the formation of MoO_XS_{4-X}, (3) the formation of MoS_3 and (4) the thermal decomposition of MoS_3 to form MoS_2. The reaction process for the synthesis of MoS_2 was expressed as follows:

$$CS(NH_2)_2 + H_2O \rightarrow NH_3 + CO_2 + H_2S \quad (1)$$

$$(NH_4)_6Mo_7O_{24} + H_2S \rightarrow MoO_xS_{4-x} + NH_3 + H_2O \quad (2)$$

$$MoO_xS_{4-x} + H^+ \rightarrow MoS_3 + H_2O \quad (3)$$

$$MoS_3 \xrightarrow{\Delta} MoS_2 \quad (4)$$

The overall reactions could be expressed as (5):

$$(NH_4)_6Mo_7O_{24} + CS(NH_2)_2 + H^+ + H_2O \rightarrow MoS_2 + CO_2 + NH_3 \quad (5)$$

3.2 Catalyst characterization

The crystal structure and phase purity of MoS_2 catalysts prepared under different pressures and pH value are characterized by XRD. As shown in Fig. 1, the catalysts prepared under the same pH

value but different pressure presented similar XRD patterns, indicating that the pressure had little effect on the crystal structure. All of the catalysts displayed some peaks at 2θ=14°, 33°, 36° and 59°, matching well with the reflection peaks for the (0 0 2), (1 0 0), (1 0 3), (1 1 0) planes of hexagonal structure of MoS_2 (JCPDS card no. 37-1492).[36, 37] It is noteworthy that (002) peak of these catalysts significantly broadened and its intensity decreased with pH value, suggesting its small crystallite size and a small number of layers in direction of the z-axis perpendicular to the atomic layers, but the reaction pressure had little effect on the intensity of peak at 2θ=14°. Mo-S-1 and Mo-S-4 showed some diffraction peaks at 2θ= 20°, 27°, 43° and 55°, corresponding to MoO_3,[38] which meant that Mo was not completely converted into MoS_2 under the condition of 200 °C, pH 1.4 and 12 h. When the pH value decreased to 0.9, not any MoO_3 was detected in the catalyst by XRD characterization. In addition, Mo-S-1, Mo-S-2, Mo-S-3 and Mo-S-4 showed a weak diffraction peak at 2θ=9°. This peak was related to the diffraction of adjacent few-layered MoS_2 sheets [39] and the strong intensity of this peak in the XRD patterns of Mo-S-1 and Mo-S-4 might be resulted from the high pH value.

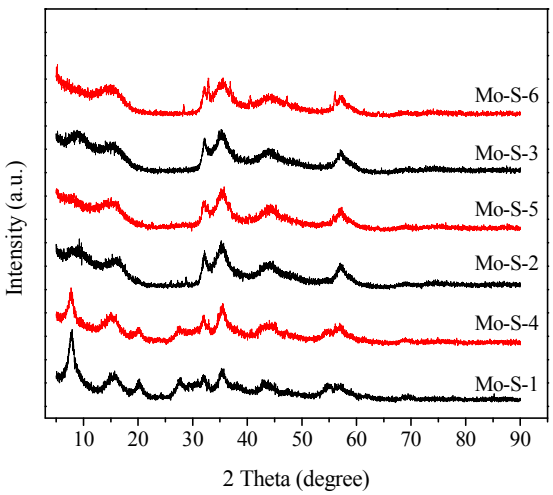

Fig. 1 XRD patterns of MoS_2 prepared under different pressures and pH values

The specific surface area and pore size distribution of MoS_2 catalysts were measured using Brunauer–Emmett–Teller (BET) and Barrett–Joyner–Halenda (BJH) method, respectively, as shown in Fig. 2 and Fig. S1 (ESI†). The samples prepared with different pressure (2.3 MPa and 1.5 MPa) almost showed the same change trend on N_2 adsorption-desorption isotherm and pore size distribution. According to the IUPAC classification,[40] these three catalysts exhibited a type IV isotherm, characterizing a typical mesoporous materials.[41, 42] The pore size distribution of Mo-S-5 and Mo-S-6 revealed these two catalysts possessed two kinds of mesoporous size, but the bimodal mesoporous peak for Mo-S-4 was not very obvious. Mo-S-6 showed a narrower pore size distribution than Mo-S-5. The most pores size of Mo-S-6 were in mesoporous range with two peak centered at 2.5 nm and 9.1 nm, where the big pores might originate from the gap between MoS_2 particles. This indicated that low pH value was beneficial to obtain bimodal mesoporous MoS_2 with a narrow peak distribution.

The surface area, pore volume and pore diameter of MoS_2 catalysts prepared under different pH values and pressures are listed in Table 2. The specific surface areas were measured to 64.5, 92.5 and 112.0 m^2/g for Mo-S-1, Mo-S-2 and Mo-S-3, respectively. This suggested that the specific surface area of MoS_2 increased with the decrease of pH value. However, the specific surface areas of Mo-S-4, Mo-S-5 and Mo-S-6 was 97.7, 170.0, 187.7 m^2/g, respectively, which was higher than that of the catalyst prepared under 2.3 MPa at the same pH value. This displayed that high pressure had a negative effect on the specific surface area of MoS_2 due to the acceleration of particles aggregation at high pressure. The effect of pH value and pressure on the pore volume was not obvious. Mo-S-5 presented the highest pore volume (0.8 cm^3/g). These samples also had micropore volumes (Table 1s, ESI†), but the mesoporous was much more important than micropore on the view of mass transfer resistance for *p*-cresol and product molecules. Moreover, compared with the total pore volume, the micropore volume was much smaller, which could be neglected.

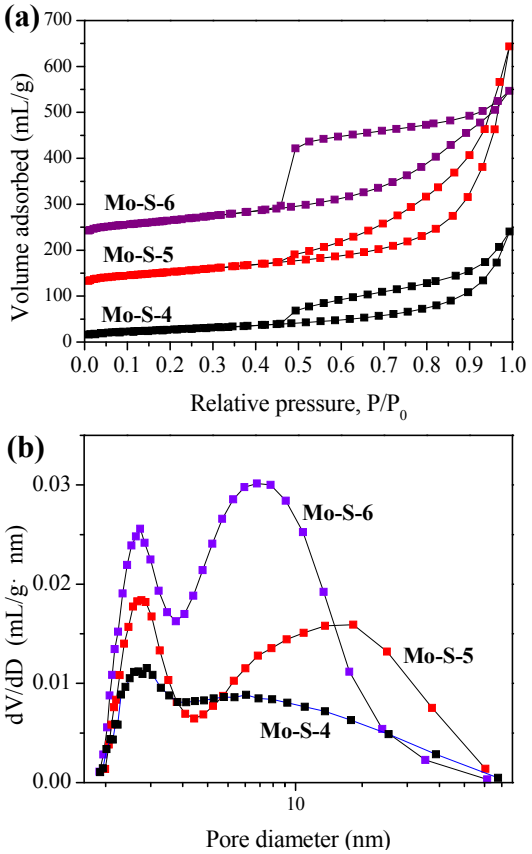

Fig. 2. Nitrogen adsorption–desorption isotherms (a) and pore size distribution (b) of Mo-S-4, Mo-S-5 and Mo-S-6

Fig. 3 shows the morphologies of MoS_2 synthesized in different pH value and pressure at 200 °C for 12 h. These MoS_2 were composed of the sheet-like shape due to the laminar growth habit of the molybdenum sulfide. Mo-S-1 presented some flower-like particles in the SEM image, which resulted from the retarding growth along the (00l) direction at high pH value.[43] After the pH value decreased, many secondary particles with smaller size made up of ultrathin nanosheets were formed and aggregated together, and the nanosheet shape of MoS_2 synthesized at lower

pH value became not clear as that of Mo-S-1. This phenomenon could be explained by following. According to the formation mechanism of MoS_2, the acid accelerated the hydrolysis of $CS(NH_2)_2$ and the formation of MoO_xS_{4-x} and MoS_3. Consequently, the formation rate of MoS_2 was enhanced at strong acid environment, promoting the growth along the (00l) direction and then weakened the nanosheet structure.

Table 2 Physical properties of MoS_2 prepared under different pressures and pH values

Catalysts	Surface area (m^2/g)	Pore volume (cm^3/g)	Pore size (nm)	Number of layers
Mo-S-1	64.5	0.2	2.3	4.5
Mo-S-2	92.5	0.5	2.4, 12.6	4.9
Mo-S-3	112.0	0.6	2.5, 10.6	5.0
Mo-S-4	97.7	0.4	2.6	4.6
Mo-S-5	170.0	0.8	2.7, 10.7	3.6
Mo-S-6	187.7	0.5	2.5, 9.1	4.1

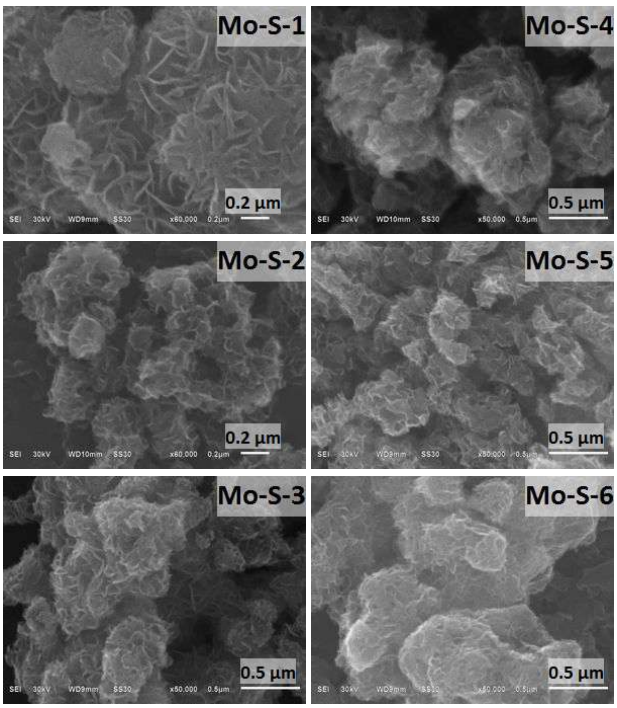

Fig. 3 SEM images of MoS2 prepared under different pressures and pH values

TEM characterization was employed to further study the microstructure of these prepared MoS_2 nano-sheets, as shown in Fig. 4. Their TEM images displayed some random groups of parallel dark thread-like fringes with 2-9 layers in the stacks. The interlayer separation between the MoS_2 layers was about 0.61 nm, which was consistent with the theoretical spacing for (002) planes of the hexagonal MoS_2 structure.[31, 32] The average layer number of MoS_2 were statistically analyzed and listed in Table 2. The average number of layers in the stacks of Mo-S-1, Mo-S-2, Mo-S-3, Mo-S-4, Mo-S-5 and Mo-S-6 was 4.5, 4.9, 5.0, 4.6, 3.6 and 4.1, respectively, but there was not any clear regularity for the layers number with the change of pressure and pH value.

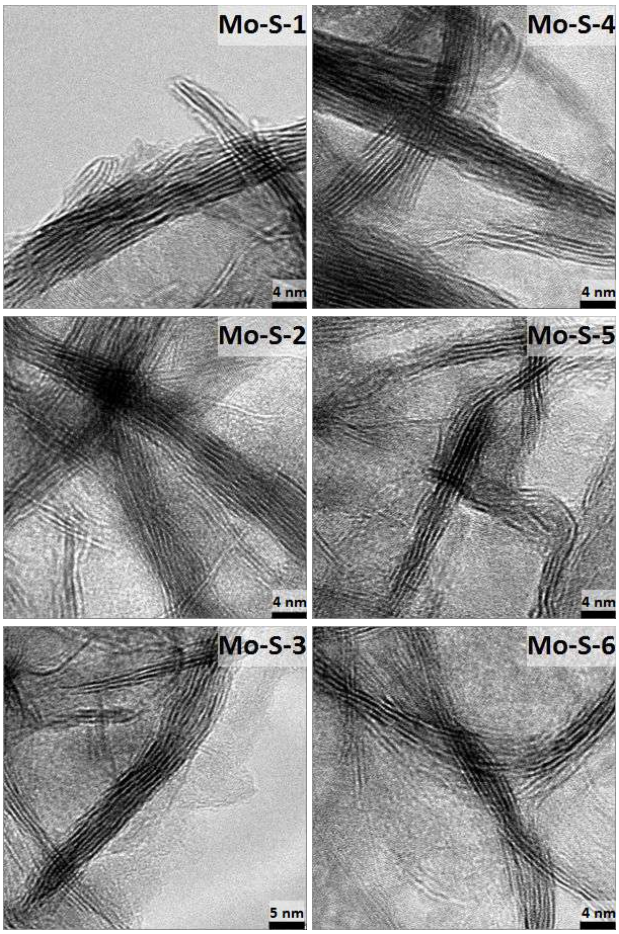

Fig. 4 TEM images of MoS_2 prepared under different pressures and pH values

3.3 HDO activity of MoS_2 in the HDO of p-cresol

To compare commercial MoS_2 (Mo-S-C) with the prepared MoS_2 on the catalytic activity, we recorded the change of conversion and products selectivity versus reaction time in the HDO of *p*-cresol on these two catalysts at 300 °C, as shown in Fig. 5. The oxygen-free products were toluene, methylcyclohexane and 3-methylcyclohexene, and no oxygen-containing compound was detected in the products, showing their high deoxygenation activity. It had reported that the HDO of phenols on sulfides proceeded with two parallel routes, including direct deoxygantion (DDO) and hydrogenation-dehydration (HYD).[3, 26] Toluene and methylcyclohexane were the final products for these two routes and 3-methylcyclohexene acted as an intermediate in the HYD route. Fig. 5 indicated that both methylcyclohexane and toluene concentrations increased with *p*-cresol conversion, but toluene concentration was much larger than the total concentration of methylcyclohexane and methylcyclohexane during the whole reaction, suggesting that the DDO was the dominate route in the HDO of *p*-cresol on MoS_2 catalyst, which agreed well with the previous investigations.[25-27] Fig. 5 also obviously showed that Mo-S-1 had higher HDO activity than Mo-S-C. After reaction at 300 °C for 10 h, the conversion of *p*-cresol on Mo-S-C was only 29.8% with a deoxygenation degree of 26.7%, but the conversion and deoxygenation degree on Mo-S-1 was 88.1% and 86.4%, respectively, exhibiting the superiority of this method for the

preparation of MoS_2 catalyst.

The conversion, product distribution, HYD/DDO and deoxygenation degree in the HDO of *p*-cresol on these catalysts prepared at different pH value and pressure at 300 °C for 4 h are listed in Table 3. The results indicated that the preparation conditions of MoS_2 had a great influence on its activity. The *p*-cresol conversion on these catalysts increased in the order of Mo-S-1 (48.3%) < Mo-S-2 (75.5%) < Mo-S-3 (93.5%) and Mo-S-4 (76.1%) < Mo-S-5 (89.1%) < Mo-S-6 (99.9%). Due to the high deoxygenation activity of MoS_2, there was not any oxygen-containing compound in products and the deoxygenation degree presented the same change trend as the conversion. That was, both the conversion and deoxygeantion degree increased with the pH value but decreased with the pressure in catalyst preparation. For the product distribution, toluene selectivity was the highest. The HYD/DDO value on all these prepared catalysts was lower than 1.0, especially on the catalysts prepared at high pressure, suggesting that the dominate HDO reaction route on these catalysts was DDO and the product distribution changed with the catalyst preparation conditions. Among these six catalysts, Mo-S-6 exhibited the highest HDO activity. Both the conversion and deoxygenation degree in the HDO of *p*-cresol at 300 °C for 4 h reached to 99.9%.

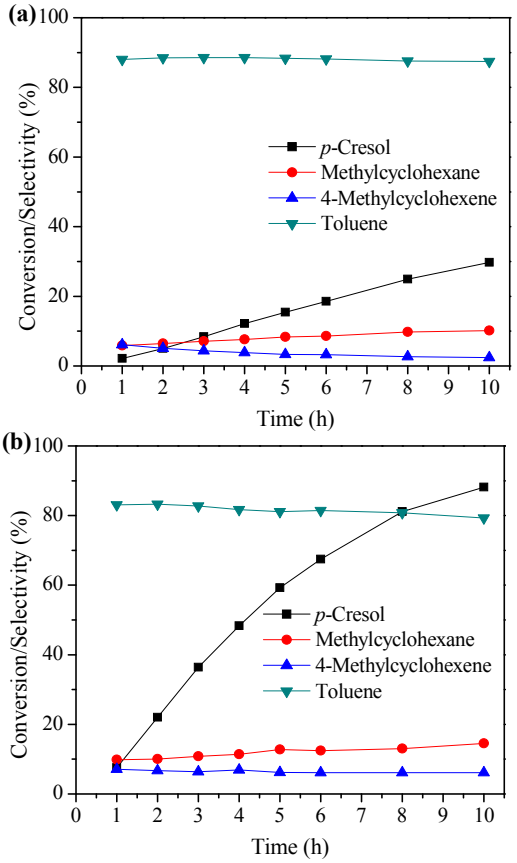

Fig. 5. The changes of p-cresol conversion and products selectivity versus reaction time on (a) Mo-S-C and (b) Mo-S-1 at 300 °C

As expected, the different conversion on these catalysts was related to their structure properties, which could be explained as followings. Firstly, the N_2 physisorption results showed that the surface area increased with the decrement of pH value. The larger surface area of the catalyst contributed more effective active sites for the HDO reaction. Consequently, the conversion on the catalyst with larger surface area was higher. However, according to the results reported by B. Yoosuk,[26] the HDO catalytic activities of MoS_2 catalysts might not be directly related to its surface area. As shown in Table 3, the conversion on Mo-S-5 and Mo-S-6 was 89.1% and 99.9%, respectively. Here, the surface area of these two catalysts were very close. But the pore size distribution showed that Mo-S-6 possessed narrower bimodal peaks and more big pores than Mo-S-5. These big pores had appropriate channels, which minimized the mass transfer resistance for *p*-cresol and product molecules and then enhanced the HDO activity. This similar result had also been reported in previous study,[28] where concluded that the catalyst with bimodal mesoporous structure presented the higher HDS activity than that of catalyst with mono-modal structure.

Table 3 Effects of pH values and pressures in the catalyst preparation on the structure of MoS2 and their catalytic activity in the HDO of p-cresol at 300 °C for 4 h

Catalysts	Mo-S-1	Mo-S-2	Mo-S-3	Mo-S-4	Mo-S-5	Mo-S-6
Conversion (mol %)	48.3	75.5	93.5	76.1	89.1	99.9
Products distribution (mol %)						
Methylcyclohexane	11.4	10.7	9.8	11.8	34.7	26.6
3-Methylcyclohexene	6.9	3.8	3.1	4.4	9.8	7.2
Toluene	81.7	85.5	87.1	83.8	55.5	66.2
HYD/DDO	0.22	0.17	0.15	0.19	0.80	0.51
D. D., wt %	44.6	72.6	92.5	73.3	87.7	99.9

Table 3 showed that the selectivity of toluene produced by DDO route on Mo-S-4, Mo-S-5 and Mo-S-6 was 83.8%, 55.5% and 66.2%, respectively. But what leaded to this difference? This mainly depended on its microstructure. Rim−Edge model, proposed by Daage M et al.,[44] was a generally accepted model to reveal the relation between products distribution and the microstructure of MoS_2 catalyst. In this model, MoS_2 was described as stacks of several layers, the top and bottom layers were defined as rim sites and the others are defined as edge sites. Daage M. et al. [44] had claimed that the direct desulfurization (DDS) reaction proceeded on both rim and edge sites while the hydrogenation reaction only occurred on rim site in the HDS of dibenzothiophene. Associated the average number of layers in the stack of MoS_2 in Table 2 with the toluene selectivity in Table 3, HYD/DDO was the lowest on Mo-S-3 with average layer number of 5.0 but the highest on Mo-S-5 with average layer number of 3.6. Hence, the larger the average layer number of MoS_2 possessed, the higher toluene selectivity was in the HDO of *p*-cresol, which was well consistent with the Rim−Edge model. The two separate routes (DDO and HYD) in the HDO of *p*-cresol on MoS_2 catalysts was related to the two different adsorption (orientation adsorption and co-planar position adsorption) of *p*-cresol on MoS_2 active sites at the beginning.[10, 45] Therefore, it could conclude that rim sites adsorbed *p*-cresol molecules via co-planar position, while edge sites adsorbed *p*-cresol molecules via vertical orientation, producing methylcyclohexane and toluene as the final products after HDO reaction.

It had reported that the HDO reaction temperature played a

significant role to phenols conversion and products distribution and high temperature was beneficial to the DDO route while low temperature was favorable for hydrogenation route.[7, 27, 46] Consequently, the effect of reaction temperature on the conversion and products distribution was studied by using the HDO of *p*-cresol on Mo-S-7, as shown in Fig. 6. *p*-Cresol conversion increased with reaction temperature and the deoxygeantion degree increased from 62.9% at 275 °C to 90.2% at 325 °C, which indicated that the HDO of *p*-cresol was controlled by kinetics. But this did not mean that deoxygeantion degree would be increased with the reaction temperature all the time because there existed an exothermic reversible reaction equilibrium in this HDO reaction according to the thermodynamic calculation.[46] For the product distribution, the total selectivity of methylcyclohexane and methylcyclohexene produced by HYD route was increased firstly and then decreased when the reaction temperature raised from 275 °C to 325 °C. This change on selectivity could be explained with the following reasons. The Gibbs free energy for the hydrogenation of *p*-cresol to 4-methylcyclohexanol was calculated to be –0.7, 1.5 and 3.8 kcal/mol at 275, 300 and 325 °C, respectively. This suggested that the hydrogenation of *p*-cresol became hard with the increase of reaction temperature, leading to the decline of HYD route selectivity. On the other hand, this hydrogenation reaction was related to the hydrogen absorbed on the catalyst. Although the total pressure was fixed to 4.0 MPa with hydrogen, the solubility of hydrogen in the solvent decreased with temperature and then decreased the available H_2 on the catalyst surface.[47] Maybe the required H_2 on the catalyst surface for the hydrogenation of *p*-cresol at 300 °C is sufficient, but it became insufficient when the temperature increased to 325 °C, and then lowed the methylcyclohexane selectivity.

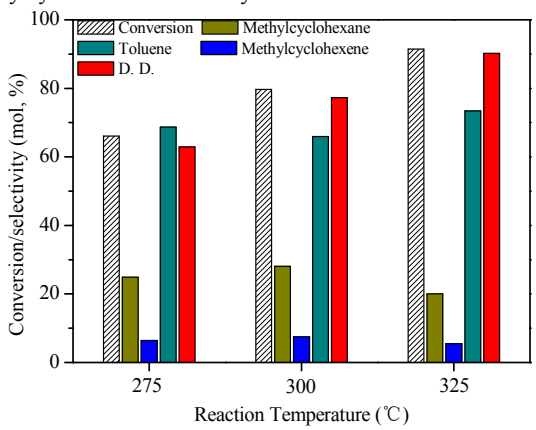

Fig. 6 The effect of reaction temperature on the conversion and products distribution in the HDO of p-cresol on Mo-S-7

To further study the effect of surface area, pore size distribution and layers in the stack of MoS_2 catalyst on its activity, we prepared MoS_2 catalysts at 240 °C for different time and then applied them into the HDO of *p*-cresol. The surface area of MoS_2 catalysts and their catalytic activities are shown in Table 4. The surface area increased firstly and then decreased with preparation time. Mo-S-8 had the highest surface area (217.0 m^2/g). This suggested that appropriate preparation time was helpful to obtain MoS_2 with large surface area. The conversion on Mo-S-7 was 70.0% at 300 °C for 5 h, which increased to 89.3% on Mo-S-8 and then decreased to 62.9% on Mo-S-9. This trend of conversion on MoS_2 was agreement with its surface area, meaning that higher surface area was beneficial to enhance the catalyst activity. However, comparing with MoS_2 prepared at 200 °C such as Mo-S-5, Mo-S-8 had higher surface area but exhibited almost same conversion in the HDO of *p*-cresol. This suggested that the high conversion might be related to other factors, except the surface area. Fig. 7 displays the comparison of Mo-S-5 and Mo-S-8 on pore size distribution. Mo-S-8 had a bimodal mesoporous, but its large pore peak was very broad, being in range of 4.2 nm to 220 nm. In contrast, Mo-S-5 exhibited narrow large pore distribution peak. Hence, the narrow large pore size distribution of MoS_2 was also an important factor for its catalytic activity in the HDO of *p*-cresol.

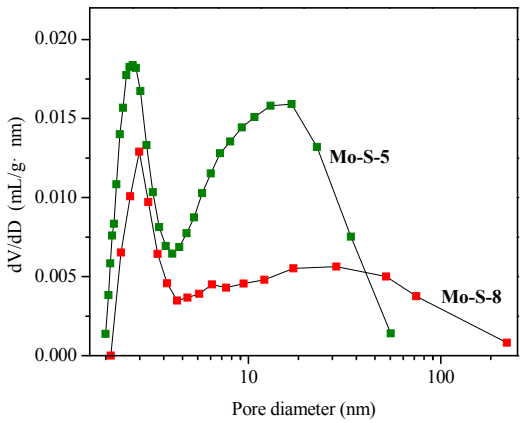

Fig. 7 Comparison of Mo-S-5 and Mo-S-8 on the pore size distribution

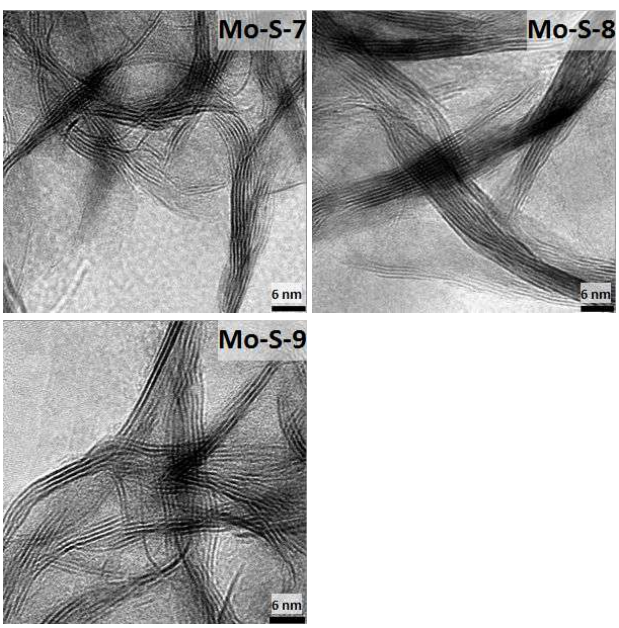

Fig. 8 HRTEM images of MoS_2 catalysts prepared by different times

Table 4 shows that Mo-S-8 had the highest direct deoxygenation activity. The toluene selectivity on Mo-S-8 was up to 84.5% and the corresponding HYD/DDO was only 0.18. The above discussion concluded that the product distribution was related to the layer number in the stacks of MoS_2 structure. To further verify this conclusion, MoS_2 catalysts prepared by different times were characterized by HRTEM and their images presented in Fig.

8. All the samples displayed the characterization of the hexagonal MoS_2 structure, but the layer number in the stacks of MoS_2 decreased in the order of Mo-S-8 > Mo-S-9 ≈ Mo-S-7. The toluene selectivity in the HDO of *p*-cresol on Mo-S-7 and Mo-S-9 was 66.0% and 68.7%, respectively, which was lower than that on Mo-S-8. This verified that the higher direct deoxygenation activity of MoS_2 depended on the more layers in its stacks again.

Until now, unsupported MoS_2 catalyst had been synthesized by several preparation methods such as mechanical activation method, *in situ* decomposition of soluble Mo precursors, exfoliation method and hydrothermal method, resulting in different HDO activity. In the HDO of *p*-cresol, Wang et al.[48] had reported that the conversion on Mo-W-S prepared by mechanical activation method was only 50% under the conditions of *p*-cresol/MoS_2 weight ratio of 13.9, 300 °C, 3.0 MPa pressure and 5 h. Yang et al.[46] had reported that *p*-cresol conversion on MoS_2 derived from the *in situ* decomposition of ammonium heptamolybdate tetrahydrate or exfoliated MoS_2 was 52% and 75% under the conditions of *p*-cresol/MoS_2 weight ratio of 14.4, 350 °C, 2.8 MPa pressure and 7 h, respectively. B. Yoosuk et al.[49] had reported that the conversion in the HDO of phenol on MoS_2 synthesized by hydrothermal method using ammonium tetrathiomolybdate as raw material was 71% under the conditions of phenol/MoS_2 weight ratio of 4, 350 °C, 2.8 MPa pressure and 1 h. However, in this study, MoS_2 was prepared from ammonium heptamolybdate by hydrothermal method. After optimizing the synthesis conditions such as temperature, pH value, reaction time and pressure, MoS_2 with bimodal mesoporous nanosheet was prepared and exhibited high HDO activity. *p*-Cresol conversion reached to 99.9% with a deoxygenation degree of 99.9% under the conditions of *p*-cresol/MoS_2 weight ratio of 22.5, 300 °C, 4.0 MPa pressure and 4 h. In addition, this method was easy to operate and repeat, where thiourea was used to substitute the poisonous gas H_2S. Moreover, the raw materials for the preparation of MoS_2 were common and cheap. All of these indicated the superiority of this method for the preparation of MoS_2 with high HDO activity. For the HDO reaction, it was inevitable that the produced water caused to the exchange of edge sulfur atoms at reaction temperature, changing the nature of MoS_2 edge sites and then decreasing the HDO activity.[50, 51] This disadvantage might be overcome by preventing from the contact of water with catalyst. One of effect ways is to improve the hydrophobicity of sulphides catalyst. These details are still under investigation.

Table 4 Surface area of MoS_2 prepared at different times and their catalytic activities in the HDO of p-cresol at 300 °C for 5 h

Catalysts	Mo-S-7	Mo-S-8	Mo-S-9
Surface area (m^2/g)	183.6	217.0	135.2
Conversion (mol %)	70.0	89.3	62.9
Products distribution (mol %)			
Methylcyclohexane	28.1	12.5	29.9
3-Methylcyclohexene	7.5	3.0	1.4
Toluene	66.0	84.5	68.7
HYD/DDO	0.54	0.18	0.46
D. D., wt %	67.3	87.8	59.6

4. Conclusion

Bimodal mesoporous MoS_2 nanosheets with high HDO activity were prepared by optimizing the synthesis conditions such as pH value, pressure, reaction time and temperature. The pH value played an important role for the preparation of MoS_2. MoO_3 phase was detected in the sample when the pH value was 1.4. The (002) plane of MoS_2 broadened and its intensity reduced with the decrease of pH value. Low pH value was beneficial to obtain MoS_2 with a narrow bimodal peak distribution and large specific surface area. High pressure had a negative effect on its specific surface area due to the accelerated aggregation of MoS_2 particles. In the HDO of *p*-cresol, the deoxygeantion degree and HYD/DDO was 99.9% and 0.51, respectively. The high deoxygeantion degree depended on both the high surface and the narrow large pore distribution of the MoS_2 catalyst. The relation between products distribution and the microstructure of catalyst in the HDO of *p*-cresol on MoS_2 could be well explained by Rim−Edge model, where rim site adsorbed *p*-cresol molecular via co-planar position while edge site adsorbed *p*-cresol molecular via vertical orientation. The more layers in the stack MoS_2 possessed, the higher direct deoxygenation activity it exhibited.

Acknowledgment

This work was supported by National Natural Science Foundation of China (No. 21306159, 21376202) and Specialized Research Fund for the Doctoral Program of Higher Education (20124301120009).

Notes and references

[a] *School of Chemical Engineering, Xiangtan University, Xiangtan, Hunan, 411105, PR China*
[b] *National & Local United Engineering Research Center for Chemical Process Simulation and Intensification, Xiangtan University, Xiangtan 411105, P. R. China. *E-mail: wangweiyan@xtu.edu.cn (W. Y. Wang), yangyunquan@xtu.edu.cn (Y. Q. Yang)*

1. C. Liu, H. Wang, A. M. Karim, J. Sun and Y. Wang, *Chem. Soc. Rev.* , 2014, 43, 7594-7623.
2. J. Zakzeski, P. C. A. Bruijnincx, A. L. Jongerius and B. M. Weckhuysen, *Chem. Rev.* , 2010, 110, 3552-3599.
3. H. Wang, J. Male and Y. Wang, *ACS Catalysis*, 2013, 3, 1047-1070.
4. G.-H. Wang, J. Hilgert, F. H. Richter, F. Wang, H.-J. Bongard, B. Spliethoff, C. Weidenthaler and F. Schüth, *Nat. Mater.* , 2014, 13, 293-300.
5. Y. Hong, H. Zhang, J. Sun, K. M. Ayman, A. J. R. Hensley, M. Gu, M. H. Engelhard, J.-S. McEwen and Y. Wang, *ACS Catalysis*, 2014, 4, 3335-3345.
6. N. Ota, M. Tamura, Y. Nakagawa, K. Okumura and K. Tomishige, *Angewandte Chemie*, 2015, 127, 1917-1920.
7. W. Wang, L. Li, K. Wu, K. Zhang, J. Jie and Y. Yang, *Appl. Catal. A: Gen.*, 2015, 495, 8-16.
8. Y. Liu, L. Chen, T. Wang, X. Zhang, J. Long, Q. Zhang and L. Ma, *RSC Advances*, 2014, DOI: 10.1039/C4RA14304C.
9. V. N. Bui, D. Laurenti, P. Afanasiev and C. Geantet, *Appl. Catal. B: Environ.*, 2011, 101, 239-245.
10. Y. Romero, F. Richard and S. Brunet, *Appl. Catal. B: Environ.*, 2010, 98, 213-223.
11. Y. Wang, H. Lin and Y. Zheng, *Catalysis Science & Technology*, 2014, 4, 109-119.
12. J. Sun, A. M. Karim, H. Zhang, L. Kovarik, X. S. Li, A. J. Hensley, J.-S. McEwen and Y. Wang, *J. Catal.* , 2013, 306, 47-57.
13. Y. K. Lugo-Jose, J. R. Monnier, A. Heyden and C. T. Williams, *Catalysis Science & Technology*, 2014, 4, 3909-3916.

14. L. Wang, H. Wan, S. Jin, X. Chen, C. Li and C. Liang, *Catalysis Science & Technology*, 2015, 5, 465-474.
15. C. Zhao, S. Kasakov, J. He and J. A. Lercher, *J. Catal.* , 2012, 296, 12-23.
16. P. M. Mortensen, D. Gardini, H. W. P. de Carvalho, C. D. Damsgaard, J.-D. Grunwaldt, P. A. Jensen, J. B. Wagner and A. D. Jensen, *Catalysis Science & Technology*, 2014, 4, 3672-3686.
17. R. G. Kukushkin, O. A. Bulavchenko, V. V. Kaichev and V. A. Yakovlev, *Appl. Catal. B: Environ.*, 2015, 163, 531-538.
18. J. Chen, H. Shi, L. Li and K. Li, *Appl. Catal. B: Environ.*, 2014, 144, 870-884.
19. A. Infantes-Molina, E. Gralberg, J. A. Cecilia, E. Finocchio and E. Rodriguez-Castellon, *Catalysis Science & Technology*, 2015, DOI: 10.1039/C5CY00282F.
20. W. Wang, Y. Yang, H. Luo, H. Peng and F. Wang, *Ind. Eng. Chem. Res.* , 2011, 50, 10936-10942.
21. W. Wang, Z. Qiao, K. Zhang, P. Liu, Y. Yang and K. Wu, *RSC Advances*, 2014, 4, 37288-37295.
22. S. A. W. Hollak, R. W. Gosselink, D. S. van Es and J. H. Bitter, *ACS Catalysis*, 2013, 3, 2837-2844.
23. N. Yan, Y. Yuan, R. Dykeman, Y. Kou and P. J. Dyson, *Angew. Chem. Int. Ed.* , 2010, 49, 5549-5553.
24. Y. Q. Yang, C. T. Tye and K. J. Smith, *Catal. Commun.* , 2008, 9, 1364-1368.
25. C. Wang, D. Wang, Z. Wu, Z. Wang, C. Tang and P. Zhou, *Appl. Catal. A: Gen.*, 2014, 476, 61-67.
26. B. Yoosuk, D. Tumnantong and P. Prasassarakich, *Chem. Eng. Sci.* , 2012, 79, 1-7.
27. W. Wang, K. Zhang, Z. Qiao, L. Li, P. Liu and Y. Yang, *Ind. Eng. Chem. Res.* , 2014, 53, 10301-10309.
28. X. Liu, X. Li and Z. Yan, *Appl. Catal. B: Environ.*, 2012, 121–122, 50-56.
29. M. S. Rana, J. Ancheyta, S. K. Maity and P. Rayo, *Catal. Today* 2005, 109, 61-68.
30. Y. Wang, J. Wu and S. Wang, *RSC Advances*, 2013, 3, 12635-12640.
31. S.-K. Park, S.-H. Yu, S. Woo, J. Ha, J. Shin, Y.-E. Sung and Y. Piao, *CrystEngComm*, 2012, 14, 8323-8325.
32. Z. Wang, T. Chen, W. Chen, K. Chang, L. Ma, G. Huang, D. Chen and J. Y. Lee, *Journal of Materials Chemistry A*, 2013, 1, 2202-2210.
33. C. Wang, H. Lin, Z. Xu, H. Cheng and C. Zhang, *RSC Advances*, 2015, 5, 15621-15626.
34. B. E. Erickson and G. R. Helz, *Geochim. Cosmochim. Acta* 2000, 64, 1149-1158.
35. P. W. Dunne, A. S. Munn, C. L. Starkey and E. H. Lester, *Chem. Commun.* , 2015, 51, 4048-4050.
36. P. Afanasiev, C. Geantet, I. Llorens and O. Proux, *J. Mater. Chem.* , 2012, 22, 9731-9737.
37. Y. Tang, D. Wu, Y. Mai, H. Pan, J. Cao, C. Yang, F. Zhang and X. Feng, *Nanoscale*, 2014, 6, 14679-14685.
38. Y. Tian, X. Zhao, L. Shen, F. Meng, L. Tang, Y. Deng and Z. Wang, *Mater. Lett.* , 2006, 60, 527-529.
39. X. Wang, Z. Zhang, Y. Chen, Y. Qu, Y. Lai and J. Li, *J. Alloys Compd.* , 2014, 600, 84-90.
40. M. Kruk and M. Jaroniec, *Chem. Mater.* , 2001, 13, 3169-3183.
41. A. Prabhu, A. Al Shoaibi and C. Srinivasakannan, *Mater. Lett.* , 2015, 146, 43-46.
42. A. Prabhu, A. Al Shoaibi and C. Srinivasakannan, *Mater. Lett.* , 2014, 136, 81-84.
43. P. Sun, W. Zhang, X. Hu, L. Yuan and Y. Huang, *Journal of Materials Chemistry A*, 2014, 2, 3498-3504.
44. M. Daage and R. R. Chianelli, *J. Catal.* , 1994, 149, 414-427.
45. H. Wan, R. Chaudhari and B. Subramaniam, *Top. Catal.* , 2012, 55, 129-139.
46. Y. Yang, H. a. Luo, G. Tong, K. J. Smith and C. T. Tye, *Chin. J. Chem. Eng.* , 2008, 16, 733-739.
47. F. Faglioni and W. A. Goddard, *The Journal of Chemical Physics*, 2005, 122, 014704-014718.
48. C. Wang, Z. Wu, C. Tang, L. Li and D. Wang, *Catal. Commun.* , 2013, 32, 76-80.
49. B. Yoosuk, D. Tumnantong and P. Prasassarakich, *Fuel*, 2012, 91, 246-252.
50. O. I. Şenol, T. R. Viljava and A. O. I. Krause, *Catal. Today* 2005, 106, 186-189.
51. M. Badawi, J. F. Paul, S. Cristol, E. Payen, Y. Romero, F. Richard, S. Brunet, D. Lambert, X. Portier, A. Popov, E. Kondratieva, J. M. Goupil, J. El Fallah, J. P. Gilson, L. Mariey, A. Travert and F. Maugé, *J. Catal.* , 2011, 282, 155-164.

Bimodal mesopore MoS_2 nanosheet was successfully synthesized by adjusting the pH value and exhibited high HDO activity.

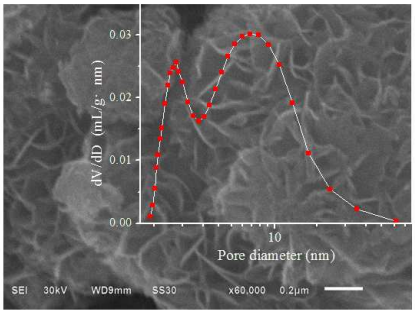

Bimodal mesoporous MoS_2 nanosheet